

Cadmium(II), Lead(II), and Zinc(II) Ions Coordination of *N,N'*-(*S,S*)Bis[1-carboxy-2-(imidazol-4-yl)ethyl]ethylenediamine: Equilibrium and Structural Studies

João G. Martins,[†] M. Teresa Barros,[‡] Rui M. Pinto,[‡] and Helena M. V. M. Soares^{*†}

[†]REQUIMTE, Departamento de Engenharia Química, Faculdade de Engenharia, Universidade do Porto, 4200-465, Porto, Portugal

[‡]REQUIMTE, Departamento de Química, Faculdade de Ciências e Tecnologia, Universidade Nova de Lisboa, 2829-516 Caparica, Portugal

ABSTRACT: The binding ability of cadmium(II), lead(II), and zinc(II) with *N,N'*-(*S,S*)bis[1-carboxy-2-(imidazol-4-yl)ethyl]ethylenediamine (BCIEE) and the structure of the formed complexes have been investigated, in aqueous solution, by potentiometry and ¹H NMR and ¹³C NMR spectroscopy for the first time. Stability constants for the cadmium, lead, and zinc complexes with BCIEE were studied by glass electrode potentiometry (GEP) at a fixed total ligand to total metal concentration ratios, varied pH values at (25.0 ± 0.1) °C, and an ionic strength of 0.1 M KCl. For the Cd-BCIEE and Pb-BCIEE systems, three species, MH₂L, MHL, and ML, were identified. For the Cd-BCIEE system, the overall stability constants values are 20.63 ± 0.02, 14.78 ± 0.01, and 8.22 ± 0.02, respectively. For the Pb-BCIEE system, the overall stability constants values are 19.71 ± 0.02, 13.78 ± 0.02, and 6.63 ± 0.02, respectively. For the Zn-BCIEE system, two species, ZnH₂L and ZnL, were identified, and the overall stability constants values are 21.84 ± 0.03 and 10.77 ± 0.04, respectively. In addition, the combined analysis of ¹H NMR and ¹³C NMR spectroscopic data enabled the establishment of the coordination modes of the metal complexes between BCIEE and the Cd(II) or Zn(II) metal ions.

1. INTRODUCTION

Transition metal chelators are broadly used in a variety of consumer products and processes, for example, in the pulp and paper, textile, cosmetic, pharmaceutical, food, and detergent industries, as well as in the remediation of metal-contaminated soils, sediments, and sludges. The molecular design requirements for an effective chelator (i.e., hexadentate ligand derived from a diamine with carboxylate or phosphonate moieties) are well-known and exemplified in current commercially available materials, such as the aminopolycarboxylate (APCA) [ethylenediaminetetracetic acid (EDTA), diethylenetriaminepentacetic acid (DTPA), etc.] or aminopolyphosphonate [ethylenediamine tetra(methylene phosphonic acid) (EDTMP), diethylenetriamine-penta(methylene-phosphonic acid) (DETPMP), etc.] acids. These chelators are, however, nonbiodegradable, and their accumulation in the environment has been the cause of a great deal of concern. Therefore, there is a pressing requirement to replace EDTA and similar ligands with readily biodegradable alternatives.

The search for new complexes able to replace the older generation of chelating agents has received a great deal of attention in recent years. Synthesis,^{1,2} complexation,^{3–7} and biodegradation⁸ studies of potential biodegradable chelating agents have been reported in the literature. One of these candidates is the [*S,S*]-stereoisomer of ethylenediaminedisuccinic acid, *S,S*-EDDS, and its biodegradability in domestic sludge has been demonstrated.⁹

In recent years, our group has been involved in the development of environmentally friendly complexing agents. During our ongoing work, several potential biodegradable compounds were

synthesized, and the metal complexation properties were studied.^{10–12} These compounds are ethylenediamine disubstituted derivatives with two secondary nitrogen atoms in the molecule, which are potentially biodegradable.¹³ These ligands were synthesized using units of the enantiopure L-amino acid, the isomeric form more abundant in living organisms.¹⁴ These facts altogether point out that these compounds have the required structural characteristics as potential green chelating agents.

Recently, *N,N'*-(*S,S*)bis[1-carboxy-2-(imidazol-4-yl)ethyl]ethylenediamine (BCIEE) (Figure 1) was synthesized.¹⁵ Complexation studies revealed that BCIEE acts as a strong complexing agent for Cu(II), Co(II), and Ni(II) ions.¹² Under this context, BCIEE was synthesized based on the method described by Miyake et al.,¹⁵ and the formation constants of the complexes, in aqueous solution, with BCIEE and Cd(II), Pb(II), and Zn(II) metal ions were determined by potentiometry. Then, spectroscopic properties of the Cd(II) and Zn(II) complexes were characterized by means of nuclear magnetic resonance techniques (¹H NMR and ¹³C NMR). Further work related to the biodegradability of BCIEE should be carried out.

2. MATERIAL AND METHODS

2.1. Potentiometric Measurements. The potentiometric titrations were performed with a personal computer (PC)-controlled system as previously described.¹⁰ The ionic strength of

Received: July 25, 2010

Accepted: January 3, 2011

Published: February 04, 2011

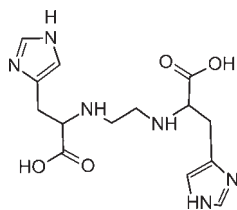


Figure 1. Structure of N,N' -(S,S)-bis[1-carboxy-2-(imidazol-4-yl)ethyl]-ethylenediamine (BCIEE).

Table 1. Experimental Conditions Used in the Determination of the Global Stability Constants in the $M-L_x-(OH)_y$ Systems, by Glass Electrode Potentiometry (GEP) and NMR Measurements, at 25 °C and $\mu = 0.1 \text{ mol}\cdot\text{L}^{-1}$ (KCl)

ligand	metal	$[L_T]:[M_T]$	$\frac{[M_T]}{\text{mol}\cdot\text{L}^{-1}}$	pH range
GEP	Cd	1	$1.0\cdot 10^{-3}$	2.0–11.5
		2	$1.0\cdot 10^{-3}$	
	Pb	1	$1.0\cdot 10^{-3}$	
		2	$1.0\cdot 10^{-3}$	
	Zn	1	$1.0\cdot 10^{-3}$	
	^1H NMR and ^{13}C NMR	Cd	2	
Zn		2	$1.0\cdot 10^{-2}$	

the solutions was adjusted to 0.1 M with KCl. The glass electrode calibration, as well as all experimental details related with the potentiometric titrations, were carried out as previously described.^{10,11}

The metal stability constants of BCIEE with metal ions Cd(II), Pb(II), and Zn(II) were all determined by direct potentiometric titrations. For all $M-(\text{BCIEE})_x-(\text{OH})_y$ systems studied, pH-potentiometric titrations were performed using fixed total ligand-to-total-metal-ion concentration ($[L]:[M_T]$) ratios over a wide pH range. The $[L_T]:[M_T]$ ratios used to characterize the $M-(\text{BCIEE})_x-(\text{OH})_y$ systems, as well as the pH range used in the potentiometric titrations, are compiled in Table 1.

The simulation and optimization procedures of the potentiometric data were performed using the ESTA program.^{16,17} The refinement operations used in potentiometry involve solving mass-balance equations, including an equation for the total proton concentration, in such a way that the computed free proton concentration, when used by the equation describing the response of the calibrated glass electrode, reproduces the experimentally recorded potential of the glass electrode as accurately as possible. This is done by minimization of an objective function, U , defined as:

$$U = (N - n_p)^{-1} \sum_{n=1}^N (E_n^{\text{obs}} - E_n^{\text{calc}})^2$$

where U is the objective function to be minimized, N is the total number of experimental titration points; n_p represents the number of parameters simultaneously optimized, E_n^{obs} is the observed electrode potential at the n th data point, and $E_n^{\text{calc}} = E^{o'} + k \log[H^+]$, where $E^{o'}$ is the electrode intercept and k the electrode calibration slope. A Gauss–Newton method is the adopted approach by ESTA to minimize U . The Hamilton R -factor, R^H , is the statistical parameter used by ESTA to reflect the

Table 2. Protonation Constants for Water, BCIEE, and Overall Stability Constants for $M(\text{II})$ Complexes with OH^- , at 25.0 °C

	equilibrium	$\log \beta$	$\frac{\mu}{\text{mol}\cdot\text{L}^{-1}}$	refs
water	$\text{H}^+ + \text{OH}^- \rightleftharpoons \text{H}_2\text{O}$	13.78	0.1	19
BCIEE	$\text{L}^{2-} + \text{H}^+ \rightleftharpoons \text{HL}^-$	9.24	0.1	18
	$\text{L}^{2-} + 2\text{H}^+ \rightleftharpoons \text{H}_2\text{L}$	16.48	0.1	18
	$\text{L}^{2-} + 3\text{H}^+ \rightleftharpoons \text{H}_3\text{L}^+$	22.52	0.1	18
	$\text{L}^{2-} + 4\text{H}^+ \rightleftharpoons \text{H}_4\text{L}^{2+}$	27.33	0.1	18
	$\text{L}^{2-} + 5\text{H}^+ \rightleftharpoons \text{H}_5\text{L}^{3+}$	30.07	0.1	18
	cadmium	$\text{Cd}^{2+} + \text{OH}^- \rightleftharpoons \text{Cd}(\text{OH})^+$	3.9	0.0
$\text{Cd}^{2+} + 2\text{OH}^- \rightleftharpoons \text{Cd}(\text{OH})_2$		7.7	0.0	19
$\text{Cd}^{2+} + 3\text{OH}^- \rightleftharpoons \text{Cd}(\text{OH})_3^-$		10.3	3.0	19
$\text{Cd}^{2+} + 4\text{OH}^- \rightleftharpoons \text{Cd}(\text{OH})_4^{2-}$		12.0	3.0	19
$\text{Cd}(\text{OH})_2(\text{s}) \rightleftharpoons \text{Cd}^{2+} + 2\text{OH}^-$		−14.35	0.0	19
zinc		$\text{Zn}^{2+} + \text{OH}^- \rightleftharpoons \text{Zn}(\text{OH})^+$	4.6	0.1
	$\text{Zn}^{2+} + 2\text{OH}^- \rightleftharpoons \text{Zn}(\text{OH})_2$	11.1	0.0	19
	$\text{Zn}^{2+} + 3\text{OH}^- \rightleftharpoons \text{Zn}(\text{OH})_3^-$	13.6	0.0	19
	$\text{Zn}^{2+} + 4\text{OH}^- \rightleftharpoons \text{Zn}(\text{OH})_4^{2-}$	14.8	0.0	19
	$\text{Zn}(\text{OH})_2(\text{s}) \rightleftharpoons \text{Zn}^{2+} + 2\text{OH}^-$	−15.5	0.0	19
	lead	$\text{Pb}^{2+} + \text{OH}^- \rightleftharpoons \text{Pb}(\text{OH})^+$	5.9	0.1
$\text{Pb}^{2+} + 2\text{OH}^- \rightleftharpoons \text{Pb}(\text{OH})_2$		10.9	0.0	19
$\text{Pb}^{2+} + 3\text{OH}^- \rightleftharpoons \text{Pb}(\text{OH})_3^-$		13.9	0.0	19
$\text{Pb}(\text{OH})_2(\text{s}) \rightleftharpoons \text{Pb}^{2+} + 2\text{OH}^-$		−16.1	0.0	23

improved agreement between the calculated and the observed data. It is given by:

$$R^H = \left[\frac{U}{\sum_{n=1}^N (E_n^{\text{obs}})} \right]^{1/2}$$

The Hamilton R -factor does not have dimensions. The ESTA software includes a proton, Z_{H} , function, defined by:

$$Z_{\text{H}} = \frac{H_T - [H^+] + [\text{OH}^-]}{L_T}$$

where $[L_T]$ and $[H_T]$ represent the total concentration of ligand and proton, respectively. This Z_{H} formation function is calculated for each datum point and plotted against pH to aid the modeling procedures. It is important to stress that the Z_{H} function can only be generated for the assumed $M-(L)_x-(\text{OH})_y$ model. This implies that one has to investigate numerous possible models and generate Z_{H} functions for all of them to select the most probable one, usually based on the observed fit of the theoretical function into the objective (experimental) one.

During the refinement operations of the different metal-BCIEE systems studied, the water and BCIEE protonation constants, as well as all known formation constants for metal hydroxide species, $M_x(\text{OH})_y$, were kept fixed (Table 2). Stability constant data for metal hydroxide species were used as they appear in Table 2. In a first attempt and for all $M-L-OH$ systems, data coming from each titration were refined with ESTA to test several models, as is shown in Table 3. Finally, when the

Table 3. Overall Stability Constants (as $\log_{10} \beta$ values) for M–BCIEE–OH Systems Determined by GEP for One Titration in 0.1 mol L^{-1} KCl at 25°C ; $M = \text{Zn(II)}, \text{Cd(II)}, \text{and Pb(II)}$; $[M_T] = 1 \cdot 10^{-3} \text{ mol} \cdot \text{L}^{-1}$

metal	Zn(II)			Cd(II)			Pb(II)		
	model I	model II	model I	model I	model II	model I	model II	model I	model II/III
$M^{2+} + L +$	NI	21.67 ± 0.02	NI	NI	20.55 ± 0.04	NI	19.80 ± 0.03	NI	19.57 ± 0.02
$2H^+ \leftrightarrow MLH_2$									
$M^{2+} + L +$	15.17 ± 0.03	R	14.44 ± 0.02	14.73 ± 0.01	14.73 ± 0.01	14.37 ± 0.04	13.75 ± 0.02	13.62 ± 0.02	13.712 ± 0.009
$H^+ \leftrightarrow MLH$									
$M^{2+} + L \leftrightarrow ML$	9.99 ± 0.04	10.67 ± 0.01	7.74 ± 0.04	8.16 ± 0.01	8.10 ± 0.06	7.66 ± 0.04	6.62 ± 0.04	6.44 ± 0.02	6.67 ± 0.01
$M^{2+} + 2L \leftrightarrow ML_2$	NI	NI	NI	NI	NI/R	NI	NI	NI	NI/R
Hamilton R-factor	0.048	0.007	0.065	0.016	0.023	0.073	0.014	0.066	0.0063
number of points	28	28	41	41	55	55	30	30	53
pH range	$4.9-6.2$	$4.9-6.2$	$5.3-7.7$	$5.3-7.7$	$4.9-7.4$	$4.9-7.4$	$5.5-7.8$	$5.5-7.8$	$5.5-7.8$

^a NI: not included; R: rejected.

Table 4. Overall Stability Constants (as $\log_{10} \beta$ Values), Refined Simultaneously for All Titrations in ESTA, for BCIEE with Cd(II), Pb(II), and Zn(II) Systems Determined by GEP in $0.1 \text{ mol} \cdot \text{L}^{-1}$ KCl at 25°C

complexes	$\log \beta$
$\text{Cd}^{2+} + \text{L}^{2-} \leftrightarrow \text{CdL}$	8.22 ± 0.02
$\text{Cd}^{2+} + \text{L}^{2-} + \text{H}^+ \leftrightarrow \text{CdLH}^+$	14.78 ± 0.01
$\text{Cd}^{2+} + \text{L}^{2-} + 2\text{H}^+ \leftrightarrow \text{CdLH}_2^{2+}$	20.63 ± 0.02
number of points	254
number of titrations/number of independent solutions	6/3
$\text{Pb}^{2+} + \text{L}^{2-} \leftrightarrow \text{PbL}$	6.63 ± 0.02
$\text{Pb}^{2+} + \text{L}^{2-} + \text{H}^+ \leftrightarrow \text{PbLH}^+$	13.78 ± 0.02
$\text{Pb}^{2+} + \text{L}^{2-} + 2\text{H}^+ \leftrightarrow \text{PbLH}_2^{2+}$	19.71 ± 0.02
number of points	259
number of titrations/number of independent solutions	6/3
$\text{Zn}^{2+} + \text{L}^{2-} \leftrightarrow \text{ZnL}$	10.77 ± 0.04
$\text{Zn}^{2+} + \text{L}^{2-} + 2\text{H}^+ \leftrightarrow \text{ZnLH}_2^{2+}$	21.84 ± 0.03
number of points	177
number of titrations/number of independent solutions	6/3

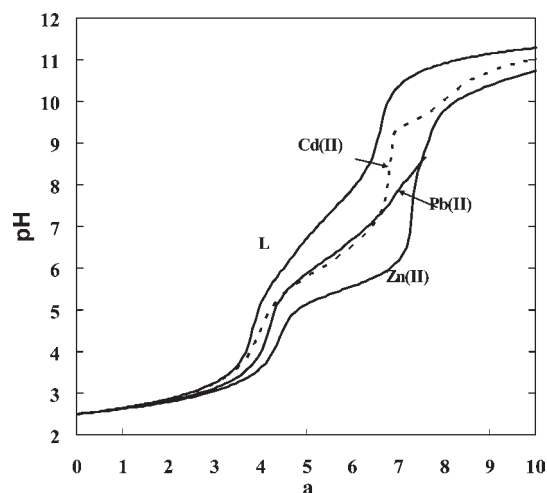


Figure 2. pH titrations of BCIEE with Zn(II), Cd(II), and Pb(II), $[L_T]:[M_T] = 1$ and $[M_T] = 1.0 \cdot 10^{-3} \text{ mol} \cdot \text{L}^{-1}$; $\mu = 0.10 \text{ mol} \cdot \text{L}^{-1}$ (KCl) and $T = 25^\circ\text{C}$. For BCIEE alone, $[\text{BCIEE}] = 1.0 \cdot 10^{-3} \text{ mol} \cdot \text{L}^{-1}$.

correct model was obtained, data coming from all titrations were introduced into ESTA, and the final overall stability constants were refined (Table 4).

2.2. NMR Measurements. The ^1H NMR and ^{13}C NMR measurements for the Cd–L–OH and Pb–L–OH systems were performed on a Bruker Avance III-400 MHz spectrometer. Measurements were made in H_2O where some drops of D_2O were added. A stock solution of each system was prepared. The pH of the batch solutions was changed by adding very small additions of a very concentrated nitric acid solution and/or saturated KOH solution with negligible variation of the total volume and measured with a combined Crison glass electrode (reference electrode Ag/AgCl). The electrode calibration was performed in a similar way as described for potentiometry.

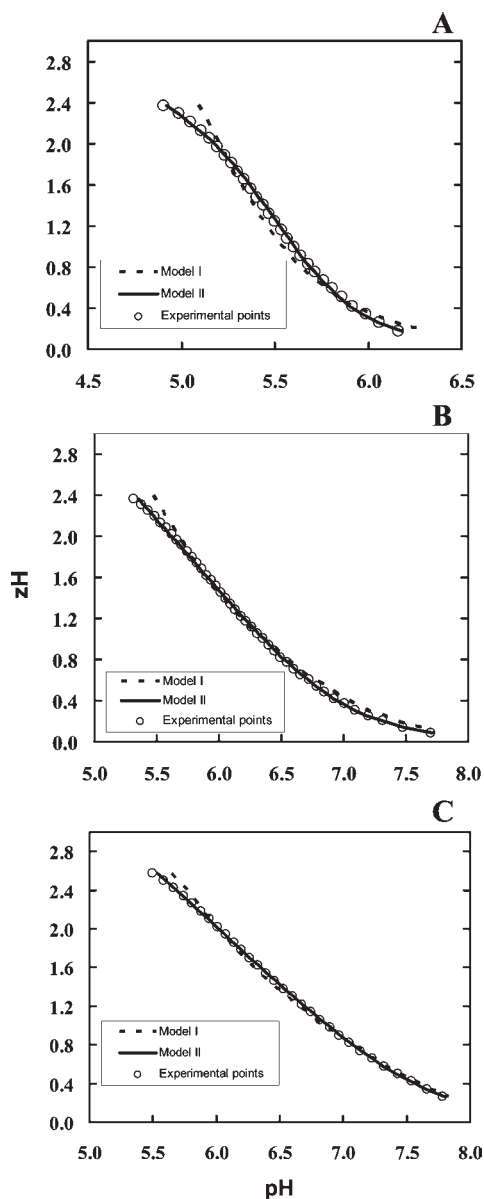


Figure 3. Z_H function for (A) Zn(II)–BCIEE–OH, (B) Cd(II)–BCIEE–OH, and (C) Pb–BCIEE–OH systems. The computed Z_H functions were calculated from the refinement operations performed for the models presented in Table 3. $[L_T]:[M_T] = 1$, $[M_T] = 1.0 \cdot 10^{-3} \text{ mol} \cdot \text{L}^{-1}$.

3. RESULTS AND DISCUSSION

The complex formation of the metal [Cd(II), Pb(II), and Zn(II)]–BCIEE–OH (M–L–OH) systems has been followed by pH-potentiometry. A comparative analysis between the experimental pH values recorded for the different metal–ligand titrations when compared with the pH titration of the ligand alone evidenced that complexation between BCIEE and the various metals begins in acidic conditions for all M–L–OH systems (Figure 2). For the Zn–L–OH system, the pH versus a (the parameter a represents the moles of base, potassium hydroxide, added per mole of ligand) curve suggests that BCIEE forms at least two species with Zn(II) (Figure 2). Less sloping pH versus a curves were recorded for the Cd–L–OH and Pb–L–OH systems (Figure 2); these results indicate the formation of weaker complexes between

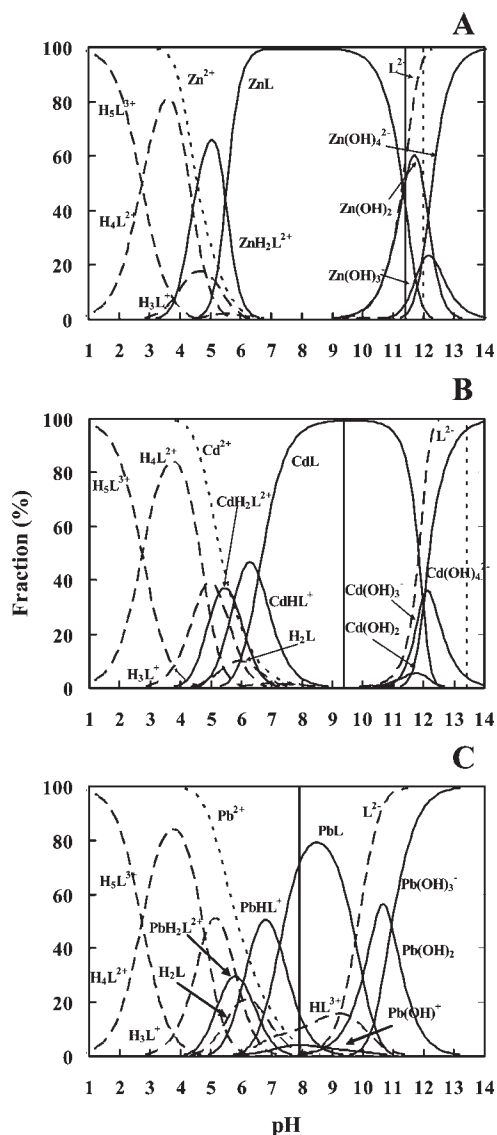


Figure 4. Species distribution diagrams computed for the various M–BCIEE–OH systems. (A) Zn–BCIEE–OH, (B) Cd–BCIEE–OH, and (C) Pb–BCIEE–OH; $[L_T]:[M_T] = 1$, $[M_T] = 1.0 \cdot 10^{-3} \text{ mol} \cdot \text{L}^{-1}$. For all M–BCIEE–OH systems, the overall stability constants of MH_xL (where $x = 0, 1$, or 2) species of model II presented in Table 3, BCIEE protonation constants, and metal hydroxide species (Table 2) were used. The vertical lines indicate $M(OH)_2$ precipitation (full line) and redissolution (dashed line).

BCIEE and Cd(II) or Pb(II) and probably the presence of more than one species.

Because BCIEE starts to complex Zn(II) at a very low pH, a variety of acidic monocomplexes, ZnH_xL , could be formed. For the refinement operations of the Zn–L–OH system, first we started with two models; the first model included the $ZnHL$, ZnL , and $ZnL_x(OH)_y$ species, and the second model included the ZnH_2L , $ZnHL$, ZnL , and $ZnL_x(OH)_y$ species. An attempt to refine all species included in the models in the whole pH range was unsuccessful. Then, models without including $ZnL_x(OH)_y$ species were refined in a narrow pH range (models I and II, Table 3). During refinement operations, $ZnHL$ was rejected in model II (Table 3). Then, the refinement operations for both simplified models (in the case of model II without $ZnHL$)

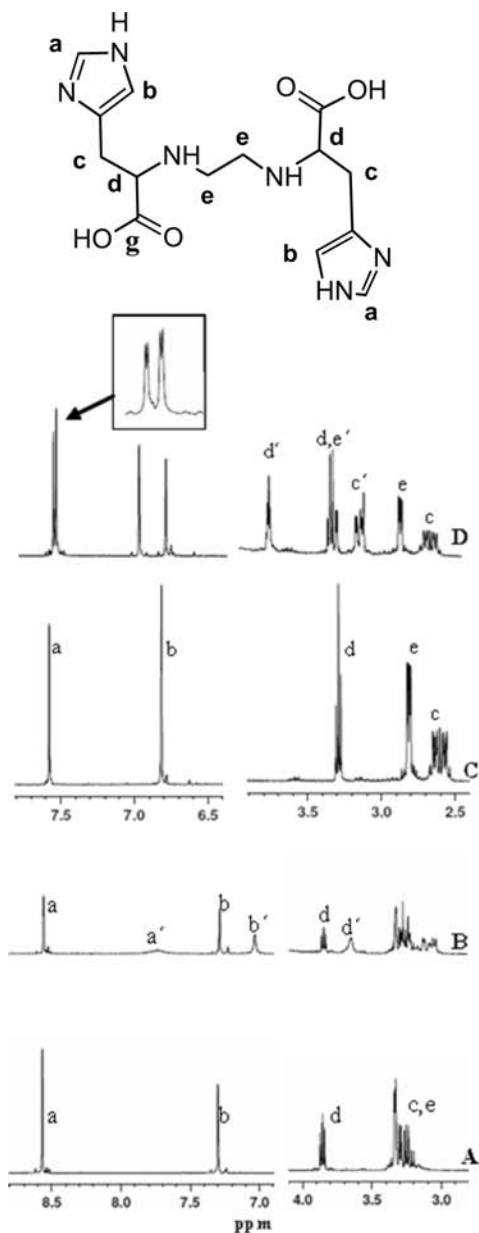


Figure 5. Parts of the ^1H NMR spectra measured for BCIEE (A and C), $[\text{BCIEE}] = 1.0 \cdot 10^{-2} \text{ mol} \cdot \text{L}^{-1}$, and for $\text{Zn}(\text{II})\text{-BCIEE-OH}$ system (B and D), $[\text{L}_\text{T}]:[\text{Zn}_\text{T}] = 2$, $[\text{Zn}_\text{T}] = 1.0 \cdot 10^{-2} \text{ mol} \cdot \text{L}^{-1}$; pH = 4 (A and B) and pH = 10 (C and D).

resulted in models with low values of the Hamilton R -factor (Table 3). From this, it was obvious that additional information was required to suggest the most likely model. For this purpose, values of the complex formation function, Z_H , were calculated for each datum point to aid in the modeling procedures (Figure 3A). The analysis of the figure showed that the experimental Z_H function (circles in Figure 3A) was reproduced fairly well with the model containing ZnL and ZnH_2L , for example, model II in Table 3.

To test the proposed model, a species distribution diagram (SDD) was generated for the experimental $[\text{L}_\text{T}]:[\text{Zn}_\text{T}]$ conditions used ($[\text{L}_\text{T}]:[\text{Zn}_\text{T}] = 1$, $[\text{Zn}_\text{T}] = 1.0 \cdot 10^{-3} \text{ mol} \cdot \text{L}^{-1}$) (Figure 4A). For this purpose, the overall stability constants of ZnL and ZnH_2L refined previously (model II, Table 3), BCIEE protonation

Table 5. ^{13}C NMR Chemical Shifts for Free Ligand and ZnH_xL ($x = 0$ or 2) Complexes at pH 4.0 and 10.0^a

pH	species	δ (ppm)						
		COO^- (g)	C_4 (f)	C_2 (a)	C_5 (b)	C_α (d)	$\text{C}_{\text{ethylene}}$ (e)	C_β (c)
4	L	172.34	127.10	127.10	117.69	61.45	43.78	25.65
	ZnH_2L , L	172.34	127.19	127.19	117.72	61.50	43.85	25.71
		179.88				60.30	46.81	28.31
10	L	181.13	136.69	136.69	115.39	64.38	46.83	30.65
	ZnL , L	180.11	134.60	135.83	115.39	63.48	46.44	29.74
				135.14		60.06	46.33	28.65
						59.97	45.92	28.60

^a Letters a, b, c, d, e, f, and g correspond to those marked in the structure of BCIEE in Figure 5.

constants, and zinc hydroxide species (Table 2) were used to build the SDD. The SDD predicts that BCIEE starts to complex with $\text{Zn}(\text{II})$ at pH 3.0 and precipitates, as $\text{Zn}(\text{OH})_2$, at pH 11.5. This last result is in agreement with the observed experimental pH value and also corroborates that $\text{ZnL}(\text{OH})_x$ species were not formed. Thus, the proposed final model should include the ZnH_2L and ZnL species. The final overall stability constants resulting from the simultaneous refinement of all titrations in ESTA are presented in Table 4.

BCIEE can act as a hexadentate ligand in aqueous solution (Figure 1). Two carboxylic groups ($\text{p}K_{\text{a}2} = 2.74$), two amine nitrogen ($\text{p}K_{\text{a}3} = 4.81$ and $\text{p}K_{\text{a}6} = 9.24$) and two imidazolyl nitrogen ($\text{p}K_{\text{a}4} = 6.04$ and $\text{p}K_{\text{a}5} = 7.21$) groups become available for complexation as the pH increases.¹⁸

If the logarithm of the H_2L protonation constant (Table 2) is subtracted from $\log \beta_{\text{ZnH}_2\text{L}}$ (Table 4), the value obtained for ZnH_2L is 5.36. This stability constant value is similar to the stability constant value of the ZnL complex formed between zinc and glycine (4.96)¹⁹ or histamine (5.22)¹⁹ but much lower than between zinc and histidine (6.51).¹⁹ On the other hand, the comparison between the $\log \beta$ value (10.77) of ZnL species (Table 4) with the $\log \beta_{\text{ZnL}_2}$ in the Zn -histidine ($\log \beta_{\text{ZnL}_2} = 12$),¹⁹ Zn -histamine ($\log \beta_{\text{ZnL}_2} = 10.7$),²⁰ and Zn -glycine ($\log \beta_{\text{ZnL}_2} = 9.19$)¹⁹ systems suggests the involvement of the two NH_2 and the two $\text{N}(\text{Im})$ groups in the Zn^{2+} coordination sphere. To find further information about the possible structure of the complexes formed, ^1H NMR and ^{13}C NMR spectra of the Zn-L system ($[\text{Zn}_\text{T}] = 1.0 \cdot 10^{-2} \text{ mol} \cdot \text{L}^{-1}$, $[\text{L}_\text{T}]:[\text{Zn}_\text{T}]$ ratio 2) were recorded at pH 4.0 and 10.0 and compared with the ^1H NMR and ^{13}C NMR spectra recorded for the ligand at the same concentration and pH values. Under these conditions, speciation distribution diagrams predicted a formation of 77.7 % of ZnH_2L at pH 4 and 100 % of ZnL at pH 10 (data not shown). At pH 10.0, ^1H NMR spectra evidence two sets of peaks of $\text{C}(2)\text{H}$ and $\text{C}(5)\text{H}$ (in Figure 5 corresponds to the ^1H NMR chemical shifts marked as a and b , respectively), when compared with the free ligand at the same pH (Figure 5). This behavior is probably due to relatively slow mutual exchange between the protonated ligand and the formed metal ion complexes.²¹ In addition, the chemical shifts corresponding to $\text{C}(\alpha)\text{H}$ and of the ethylene bridge protons (in Figure 5 corresponds to the ^1H NMR chemical shifts marked as d and e , respectively) of the complex were split and downfield shifted when compared with the free ligand (Figure 5). These results are in agreement with the histamine-like structure previously postulated. Additionally, the ^{13}C NMR spectral data for the free ligand and ZnL complex were also recorded at pH

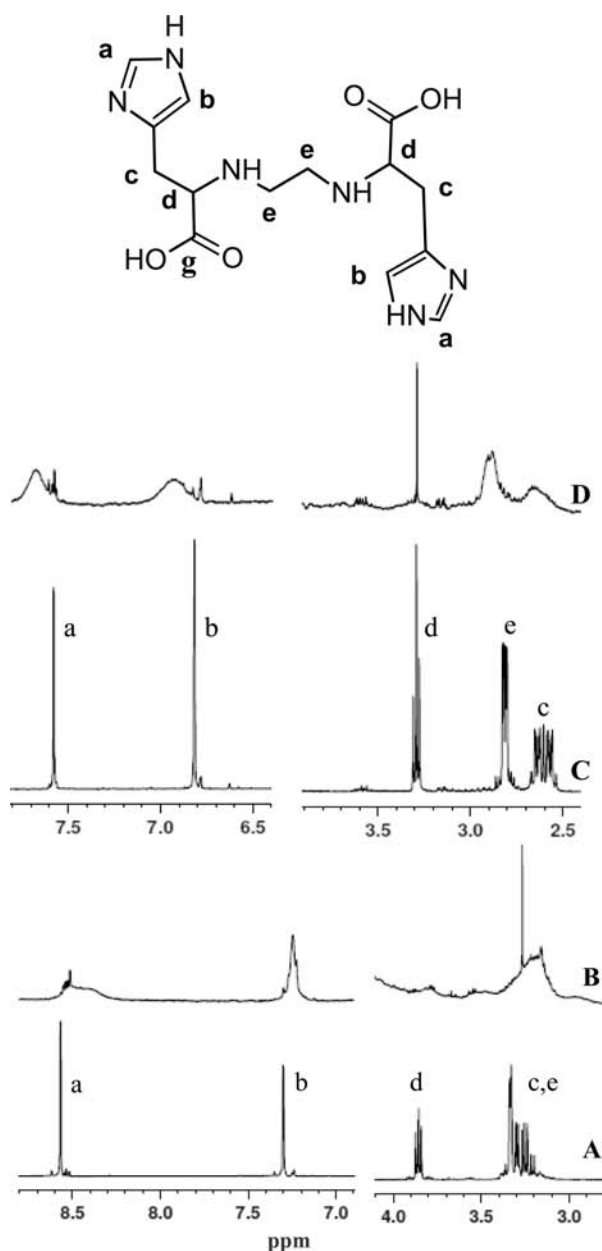


Figure 6. Parts of the ^1H NMR spectra measured for BCIEE (A and C), $[\text{BCIEE}] = 1.0 \cdot 10^{-2} \text{ mol} \cdot \text{L}^{-1}$, and for $\text{Cd(II)}-\text{BCIEE}-\text{OH}$ system (B and D), $[\text{L}_T]:[\text{Cd}_T] = 2$, $[\text{Cd}_T] = 1.0 \cdot 10^{-2} \text{ mol} \cdot \text{L}^{-1}$; pH = 4 (A and B) and pH = 10 (C and D).

10.0, and the resonance signals are given in Table 5. Table 5 shows that the chemical shifts for the carboxylic signal in the free and ZnL complex remained almost unaffected, which is evidence of no involvement of the carboxylate group in the coordination sphere of the Zn^{2+} . On the other hand, the C(2), C(α), and C(ethylene) chemical shifts were split (Table 5). The chemical shifts for C(α) signals in the complex have shown downfield shifts up to 4 ppm compared to that of the free ligand, suggesting a change upon complexation. All of these results corroborate the histamine-like coordination type of the ZnL complex. Thus, BCIEE behaves as a tetradentate ligand via the two NH_2 and the two N(Im) groups. Returning to the ZnH_2L complex, the carboxylate and ethylene carbon chemical shifts in the complex split into (179.88 and 46.81) ppm and show downfield shifts of

(7.54 and 2.96) ppm, respectively (Table 5). These results evidence the involvement of the carboxylate and NH_2 groups in the coordination sphere of the Zn^{2+} and suggest that BCIEE behaves as a bidentate ligand via COO^- and NH_2 groups. On the other hand, the ^1H NMR spectrum in the complex is evidence that the signals of C(2)H and C(5)H of the imidazole ring are split and upfield shifted suggesting a ligand change upon complexation. These results point out the involvement of the N(Im) group in the coordination sphere of the Zn^{2+} and suggest that BCIEE behaves as a bidentate ligand via N(Im) and NH_2 groups. All of these data support the coexistence of two isomeric ZnH_2L complexes (one structure constituted by one carboxylic and one amine group forming a five-membered ring and another structure constituted by one N(Im) and one amine group forming a six-membered ring); these facts are consistent with the ambidentate nature of the histidine ligand, that is, the ability to coordinate histamine-like and glycine-like modes.²⁰

For complexation studies of the $\text{Cd}-\text{L}-\text{OH}$ and $\text{Pb}-\text{L}-\text{OH}$ systems, two $[\text{L}_T]:[\text{M}_T]$ ratios, 1.0 and 2.0, were used (Table 1). First, we started the refinement operations using two models for each $[\text{L}_T]:[\text{M}_T]$ ratio: models I and II for $[\text{L}_T]:[\text{M}_T]$ ratio 1.0 and models I and III for $[\text{L}_T]:[\text{M}_T]$ ratio 2.0 (Table 3). For the $[\text{L}_T]:[\text{M}_T]$ ratio 2.0 and for both $\text{M}-\text{L}-\text{OH}$ systems, ML_2 was always rejected (model III, Table 3). In addition, the refinement operations with just the ML and MHL species (model I, Table 3) did not fit well the experimental results (Figure 4B,C) for both $\text{M}-\text{L}-\text{OH}$ systems; Figure 4B,C shows that the calculated Z_{H} functions for lower pH values (pH values < 5.8 and 6.0 for $\text{Cd}-\text{L}-\text{OH}$ and $\text{Pb}-\text{L}-\text{OH}$ systems, respectively) were above the experimental Z_{H} functions; the gap between the calculated complexation curves and the experimental points strongly supports that more species, probably MH_2L , must be included in the model for both $\text{M}-\text{L}-\text{OH}$ systems. As one can see in Table 3 and Figure 3, the inclusion of the MH_2L species in the model (model II) fitted well the experimental data and an improvement in the Hamilton R -factor was observed for both $\text{M}-\text{L}-\text{OH}$ systems. Precipitation of $\text{M}(\text{OH})_2$ was experimentally observed at pH 8.2 and 9.5 for the $\text{Pb}-\text{L}-\text{OH}$ and $\text{Cd}-\text{L}-\text{OH}$ systems, respectively, for a $[\text{L}_T]:[\text{M}_T]$ ratio of 1.0. In the absence of complexing agents, the hydrolysis of each metal ion may occur at pH 5.5 for Pb(II) and at pH 8.0 to 8.5 for Cd(II) (data not shown).¹⁹ For the $\text{Pb}-\text{L}-\text{OH}$ system, the analysis of Figure 3C shows that, up to pH 7.8, the values of the Z_{H} function did not reach negative values, which means that no $\text{PbL}(\text{OH})_x$ species were formed. For the $\text{Cd}-\text{L}-\text{OH}$ system, tentative refinement of $\text{CdL}(\text{OH})_x$ species were attempted in the pH range 7.7 to 9.0 and 7.0 to 9.6 for $[\text{L}_T]:[\text{Cd}_T]$ ratios of 1.0 and 2.0, respectively. The strategy used consisted of refining the species $\text{CdL}(\text{OH})$ assuming another model, where the values of CdH_2L , CdHL , and CdL previously refined in a lower pH range (model II, Table 3), were used as fixed values. For both $[\text{L}_T]:[\text{Cd}_T]$ ratios, ESTA always rejected the $\text{CdL}(\text{OH})$ species (data not shown).

After this modeling exercise, we concluded that the proposed final model for the $\text{Cd}-\text{L}-\text{OH}$ and $\text{Pb}-\text{L}-\text{OH}$ systems is: MH_2L , MHL , and ML . To confirm the proposed models, a SDD corresponding to the experimental conditions used ($[\text{L}_T]:[\text{M}_T]$ 1, $[\text{M}^{2+}] = 1 \cdot 10^{-3} \text{ M}$) were drawn for the $\text{Cd}-\text{L}-\text{OH}$ (Figure 4B) and $\text{Pb}-\text{L}-\text{OH}$ (Figure 4C) systems assuming the model proposed above (model II, Table 3). For this purpose, the overall stability constants of MH_2L , MHL , and ML previously refined (model II, Table 3), BCIEE protonation constants, and metal hydroxide species (Table 2) were used to build

the SDDs. The SDDs for both M–L–OH systems show that complexation starts around pH = 4, which is in agreement with the pH versus α curves (Figure 2). Additionally, the SDDs predict the occurrence of precipitation at pH = 9.3 for the Cd–L–OH system and pH = 7.9 for the Pb–L–OH system, which is also in line with what was observed experimentally. Thus, the values of the overall stability constants were refined simultaneously using all of the [LT]:[MT] ratios; the final overall stability constant values are shown in Table 4.

If the logarithm of the H₂L protonation constant is subtracted from $\log \beta_{\text{CdH}_2\text{L}}$, the obtained value for CdH₂L is 4.15. This stability constant value is similar to the stability constant value of the CdL complex formed between cadmium and glycine (4.25)¹⁹ but much lower than the value determined with histidine (5.66).¹⁹ These results suggest that BCIEE behaves as a bidentate ligand via COO[−] and NH₂ groups. However, it must be mentioned that, when we compare the stability constant value of CdH₂L (4.15) with the stability constant value of the CdL complex formed between cadmium and histamine (4.75),¹⁹ the formation of a histamine-like structure cannot be excluded. Additionally, a comparison between the magnitude of the $\log \beta$ value (8.22) of the CdL species (Table 4) with the $\log \beta_{\text{CdL}_2}$ in Cd-histidine ($\log \beta_{\text{CdL}_2} = 9.94$),¹⁹ Cd-histamine ($\log \beta_{\text{CdL}_2} = 7.91$),¹⁹ and Cd-glycine ($\log \beta_{\text{CdL}_2} = 7.77$)¹⁹ raises the hypothesis of a glycine or a histamine-like complex but clearly excludes the hypothesis of a histidine-like complex. To obtain structural information on the CdH₂L and CdL complexes, ¹H NMR (Figure 6) and ¹³C NMR spectra were recorded for [L_T]:[M_T] 1, [M²⁺] = 1 · 10^{−2} M at pH = 4.0 and pH = 10.0, respectively. At these pH values, SDD predicts the formation of (23.6 and 99.6) % of CdH₂L and CdL, respectively. No appreciable amounts of other complexes are formed at these pH values. Because the SDD (Figure 4B) predicted that the CdHL complex coexists with other species whatever the pH value considered, no attempt to obtain structural information on this species was attempted.

The analysis of the ¹H NMR spectra of the CdH₂L complex (Figure 6) reflects marked broadening of the C(2)H and C(5)H of the imidazole rings, as well as the C(α)H and ethylene bridge protons. This phenomenon refers to the presence of complexes, which are relatively slow (intermediate) mutual exchange between the protonated ligand and the formed metal ion complexes.^{21,22} These results corroborate the involvement of the N(Im) and NH₂ groups in the CdH₂L complex. Thus, we can conclude that ¹H NMR results of the CdH₂L complex corroborates the histamine-like structure. At pH 10.0, the formation of the CdL complex changes distinctly the ¹H NMR spectrum when compared with the spectrum for the free ligand; the signals of C(2)H and C(5)H of the imidazole rings, C(α)H, and ethylene bridge protons are broad (Figure 6) probably due to relatively slow mutual exchange between the protonated ligand and the formed metal ion complexes.^{21,22} These facts, together with the potentiometric data (Table 4), indicate that the deprotonation of the four amines occur in parallel with their binding to the metal ions forming macrochelates and suggests that the ligand is coordinated to the metal ions tetradentately via the two N(Im) and the two NH₂ groups.

Because of the low sensitivity observed in the case of the ¹³C NMR spectra recorded for CdH₂L and CdL complexes, no conclusions could be obtained from these results.

In the case of the Pb–L–OH system, more than one species is formed simultaneously whatever the pH value considered

(Figure 4C), which precludes a correct structural characterization of each complex. Because of this, no attempt to obtain structural characterization of lead species for this system was performed.

The analysis of SDDs for all three metal–BCIEE systems (Figure 4) evidences that metal hydroxide species are not formed in a significant extent in the pH range where the models were refined (Table 3). Thus, even though the data of the stability constant for metal hydroxide species were not corrected to be at an ionic strength of 0.1, no appreciable error was introduced in the refinement operations.

4. CONCLUSIONS

In this work, the overall stability constants of all complexes, which are formed in aqueous solution between BCIEE and cadmium(II), lead(II), and zinc(II), were studied potentiometrically at (25.0 ± 0.1) °C and an ionic strength of 0.1 M KCl. For all three systems, the complete picture of the final models was established. The following stability sequence has been obtained: zinc(II) > cadmium(II) > lead(II).

In the case of the cadmium(II) and lead(II) systems, the overall stabilities of these complexes are not high enough to prevent the hydrolysis of the metal ion, and precipitation occurs in a slightly alkaline solution.

The structure of cadmium(II)–BCIEE and zinc(II)–BCIEE complexes have also been studied by ¹H NMR and ¹³C NMR spectroscopic techniques. The results provide evidence that BCIEE acts as a tetradentate ligand involving two amino and two imidazole nitrogens in metal coordination of the CdL and ZnL complexes. Results also suggest that BCIEE behaves as a bidentate ligand [via COO[−] and N(Im) or via NH₂ and N(Im) groups], forming an equilibrium mixture of two ZnH₂L structures for the Zn(II)–BCIEE system. For the CdH₂L species, BCIEE behaves as a bidentate via one NH₂ and one N(Im) group.

■ AUTHOR INFORMATION

Corresponding Author

*H.M.V.M.S.: e-mail, hsoares@fe.up.pt; phone, +351 22 508 1650; fax, +351 22 508 1449.

Funding Sources

Financial support by FCT (Projects POCI/QUI/57891/2004 and PPCDT/QUI/57891/2004), with FEDER funds are gratefully acknowledged. One of us (J.M.) also gratefully acknowledges a grant scholarship financed under the same project. We also thank Professor Carlos Gomes from University of Porto (Portugal) for the COPOTISY program.

■ REFERENCES

- (1) Pihko, P. M.; Rissa, T. K.; Aksela, R. Enantiospecific synthesis of isomers of AES, a new environmentally friendly chelating agent. *Tetrahedron* **2004**, *60*, 10949–10954.
- (2) Lutz, M.; Pursiainen, J.; Aksela, R. Facile syntheses of novel acyclic polycarboxylic acids. *Z. Naturforsch., B: Chem. Sci.* **2005**, *60*, 408–412.
- (3) Hyvonen, H.; Orama, M.; Saarinen, H.; Aksela, R. Studies on biodegradable chelating ligands: complexation of iminodisuccinic acid (ISA) with Cu(II), Zn(II), Mn(II) and Fe(III) ions in aqueous solution. *Green Chem.* **2003**, *5*, 410–414.
- (4) Hyvonen, H.; Orama, M.; Alen, P.; Saarinen, H.; Aksela, R.; Paren, A. Complexation of N-tris[(1,2-dicarboxyethoxy)ethyl]amine

with Ca(II), Mn(II), Cu(II) and Zn(II) in aqueous solution. *J. Coord. Chem.* **2005**, *58*, 1115–1125.

(5) Hyvonen, H.; Orama, M.; Arvelac, R.; Henriksson, K.; Saarinen, H.; Aksela, R.; Parene, A.; Jakara, J.; Renvall, I. Studies on three new environmentally friendly chelating ligands. *Appita J.* **2006**, *59*, 142–149.

(6) Hyvonen, H.; Aksela, R. Complexation of [S,S,S]- and [R,S,R]-isomers of N-bis[2-(1,2-dicarboxyethoxy)ethyl] aspartic acid with Mg(II), Ca(II), Mn(II), Fe(III), Cu(II) and Zn(II) ions in aqueous solution. *J. Coord. Chem.* **2008**, *61*, 2515–2527.

(7) Hyvonen, H.; Lehtinen, P.; Aksela, R. Complexation of N-bis[2-(1,2-dicarboxyethoxy)ethyl]aspartic acid with Cd(II), Hg(II) and Pb(II) ions in aqueous solution. *J. Coord. Chem.* **2008**, *61*, 984–996.

(8) Metsarinne, S.; Ronkainen, E.; Tuhkanen, T.; Aksela, R.; Sillanpaa, M. Biodegradation of novel amino acid derivatives suitable for complexing agents in pulp bleaching applications. *Sci. Total Environ.* **2007**, *377*, 45–51.

(9) Schowanek, D.; Feijtel, T. C. J.; Perkins, C. M.; Hartman, F. A.; Federle, T. W.; Larson, R. J. Biodegradation of [S,S], [R,R] and mixed stereoisomers of ethylene diamine disuccinic acid (EDDS), a transition metal chelator. *Chemosphere* **1997**, *34*, 2375–2391.

(10) Barros, M. T.; Martins, J.; Pinto, R. M.; Santos, M. S.; Soares, H. Complexation Studies of N,N'-ethylenedi-L-cysteine with Some Metal Ions. *J. Solution Chem.* **2009**, *38*, 1504–1519.

(11) Martins, J. G.; Pinto, R. M.; Gameiro, P.; Barros, M. T.; Soares, H. M. V. M. Equilibrium and solution structural studies of the interaction of N,N'-Bis(4-imidazolymethyl)ethylenediamine with Ca(II), Cd(II), Co(II), Cu(II), Mg(II), Mn(II), Ni(II), Pb(II) and Zn(II) metal ions. *J. Solution Chem.* **2010**, *39*, 1153–1167.

(12) Martins, J.; Gameiro, P.; Barros, M. T.; Soares, H. M. V. M. Potentiometric and UV-vis spectroscopic studies of cobalt(II), copper(II) and nickel(II) complexes with N,N'-(S,S)bis[1-carboxy-2-(imidazol-4-yl)ethylenediamine]. *J. Chem. Eng. Data* **2010**, *85*, 1353–1360.

(13) Pitter, P.; Sykora, V. Biodegradability of ethylenediamine-based complexing agents and related compounds. *Chemosphere* **2001**, *44*, 823–826.

(14) O'Dowd, R. W.; Hopkins, D. W. Mineralization of carbon from D- and L-amino acids and D-glucose in two contrasting soils. *Soil Biol. Biochem.* **1998**, *30*, 2009–2016.

(15) Miyake, H.; Watanabe, M.; Takemura, M.; Hasegawa, T.; Kojima, Y.; Inoue, M. B.; Inoue, M.; Fernando, Q. Novel optically-active bis(amino acid) ligands and their complexation with gadolinium. *J. Chem. Soc., Dalton Trans.* **2002**, 1119–1125.

(16) May, P. M.; Murray, K.; Williams, D. R. The use of glass electrodes for the determination of formation constants - II. Simulation of titration data. *Talanta* **1985**, *32*, 483–489.

(17) May, P. M.; Murray, K.; Williams, D. R. The use of glass electrodes for the determination of formation constants - III. Optimization of titration data: the ESTA library of computer programs. *Talanta* **1988**, *35*, 825–830.

(18) Takemura, M.; Yamato, K.; Doe, M.; Watanabe, M.; Miyake, H.; Kikunaga, T.; Yanagihara, N.; Kojima, Y. Europium(III)-N,N'-ethylenebis(L-amino acid) complexes as new chiral NMR lanthanide shift reagents for unprotected alpha-amino acids in neutral aqueous solution. *Bull. Chem. Soc. Jpn.* **2001**, *74*, 707–715.

(19) Martell, A. E.; Smith, R. M. *NIST Standard Reference Database 46 Version 8.0, NIST Critically Selected Stability Constants of Metal Complexes Database*; U.S. Department of Commerce, National Institute of Standards and Technology: Gaithersburg, MD, 2004.

(20) Altun, Y.; Koseoglu, F. Stability of copper(II), nickel(II) and zinc(II) binary and ternary complexes of histidine, histamine and glycine in aqueous solution. *J. Solution Chem.* **2005**, *34*, 213–231.

(21) Jancso, A.; Gajda, T.; Mulliez, E.; Korecz, L. Equilibrium and solution structural study of the interaction of tri- and tetra-dentate polyimidazole ligands with transition metal ions. *J. Chem. Soc., Dalton Trans.* **2000**, 2679–2684.

(22) Jancso, A.; Kolozsi, A.; Gyurcsik, B.; Nagy, N. V.; Gajda, T. Probing the Cu(2+) and Zn(2+) binding affinity of histidine-rich glycoprotein. *J. Inorg. Biochem.* **2009**, *103*, 1634–43.

(23) Hogfeldt, E. *Stability Constants of Metal-Ion Complexes - Part A: Inorganic Ligands*; Pergamon Press: Oxford, 1982.